

To appear in The Astrophysical Journal.

## Spin–Orbit Misalignment in Close Binaries with Two Compact Objects

Vassiliki Kalogera

Harvard-Smithsonian Center for Astrophysics, 60 Garden St., Cambridge, MA 02138;  
 vkalogera@cfa.harvard.edu

### ABSTRACT

Spin–orbit misalignment in coalescing compact binaries affects their gravitational radiation waveforms. When the misalignment angles are large ( $\gtrsim 30^\circ$ ), the detection efficiency of the coalescence events can decrease significantly if the misalignment effects are not modeled. In this paper, we consider the formation of close compact binaries and calculate the expected misalignment angles after the second core collapse event. Depending on the progenitor parameters and the assumptions made about supernova kicks, we find that 30%–80% of binaries containing a black hole and a neutron star that coalesce within  $10^{10}$  yr have misalignment angles larger than  $30^\circ$  and a significant fraction of them could remain undetected. The calculations allow us to place strong constraints on the progenitors of such binaries and the kick magnitudes required for their formation. We also discuss the formation of close binaries with two black holes and the effect of non-isotropic kicks.

*Subject headings:* binaries: close — stars: supernovae — gravitation

### 1. INTRODUCTION

The prototypical double neutron star system (NS–NS) is PSR B1913+16, the first binary radio pulsar discovered 25 years ago (Hulse & Taylor 1975). Timing observations of the pulsar provided a remarkable confirmation of general relativity with the measurement of several relativistic effects including the orbital decay due to gravitational radiation (Taylor & Weisberg 1982). Since then three more such systems have been discovered, including the recently detected candidate PSR J1811-1736 (Lyne et al. 2000). The inspiral of such close NS–NS binaries continues until the orbital separation becomes comparable to the NS radii and the two stars merge on a dynamical timescale (Rasio & Shapiro 1992; Ruffert et al. 1996). Such merger events are expected to occur not only in NS–NS binaries but also in close black hole binaries, BH–NS and BH–BH. These have not yet been directly observed, but their existence is predicted by all theoretical models of binary evolution and compact object formation (Lipunov et al. 1997; Bethe & Brown 1998; Portegies-Zwart & Yungel’son 1998; Fryer et al. 1999). The final inspiral and coalescence of all 3

types of close compact binaries are major sources of gravitational waves for the laser-interferometer detectors currently under construction (LIGO, VIRGO, GEO600; see Thorne 1996 for a review).

The detection of inspiral events relies on matched filtering techniques (e.g., Schutz 1991), since the gravitational-wave signals are expected to be weak relative to the various sources of detector noise. The detection efficiency of binary coalescence depends on how extensive is the database of “search templates”, i.e., theoretically predicted inspiral waveforms calculated for large ranges of parameters, such as masses, detector location and orientation, and phase of the waves at coalescence. The magnitude and orientation of the spins of the two compact objects relative to the orbital angular momentum can also modify the inspiral waveforms because of precession driven by general relativistic spin-orbit and spin-spin couplings (e.g., Apostolatos et al. 1994). Apostolatos (1995) has pointed out that the modulation of the gravitational-wave signal can be large enough to decrease the detection efficiency significantly if non-precessing waveforms are used in the search. The loss of detection efficiency increases with (i) the mass contrast between binary components, (ii) the spin magnitude of the more massive component, and (iii) the spin misalignment from the angular momentum axis. Even for maximally rotating NS, it appears that an unmodulated family of templates would be sufficient for the detection of NS–NS inspiral events. However, in the case of BH–NS binaries (typical mass ratio  $\sim 0.1$ ) with maximally rotating BH, such a template family would be insufficient for more than 50% of all binary orientations if the spin tilt angle exceeds  $30^\circ$ – $40^\circ$  and for *all* binary orientations if the spin tilt angle exceeds  $50$ – $60^\circ$  (Apostolatos 1995).

The ranges of parameters that the template database can realistically cover is limited by the computational cost of computing a large number of cross-correlations between templates and data. The range of spin properties (magnitudes and orientations) is further limited by the computational cost associated with calculations of precession-modulated templates. Given these limitations it is important to examine (i) whether it is necessary, based on astrophysical considerations, to worry about the possibility of a significant misalignment, and (ii) how extended a range of tilt angles should be covered by the precessing templates.

In this paper we focus on the formation of close BH–NS binaries and we determine the spin orientation of the BH at the time of their formation. The evolution of BH–NS binary progenitors *prior* to the explosion associated with the NS formation in the binary involves mass transfer phases, which are expected to align the spins of both the BH and the NS progenitor. Any spin tilt angle is therefore expected to be introduced by the supernova (SN) explosion that forms the NS. Mass loss alone cannot misalign the two axes. However, there is now growing evidence that asymmetric kicks are imparted to NS at birth (see Fryer et al. 1999 and references therein). In fact, as we show in § 3.1, the formation of a coalescing BH–NS binary *requires* a significant NS kick. Depending on the kick magnitude and direction, the plane of the post-SN orbit can be tilted relative to the pre-SN plane and hence the BH spin axis. We consider a set of BH–NS progenitors (defined by the NS progenitor mass and the pre-SN orbital separation) and calculate the theoretically expected distributions of BH spin tilt angles for a number of isotropic kick magnitude distributions. The results are most sensitive to the pre-SN orbital separation and less

sensitive to the assumed kick distribution. A range of 30%–80% of BH–NS binaries are found to have tilt angles in excess of  $30^\circ$ . A discussion of the model assumptions is presented in § 2.1 and the analysis of the asymmetric explosion is described in § 2.2. Our results, along with a detailed parameter study are presented in § 3. The effects of non-isotropic kicks are analyzed in § 4. The significance of these results for the expected gravitational wave detection efficiencies as well as our expectations for close BH–BH binaries are discussed § 5.

## 2. METHODS

### 2.1. Assumptions about Binary Progenitors

Our current understanding of BH–NS binary formation (with a  $\sim 10 M_\odot$  BH) leads to an evolutionary history similar to that of NS–NS binaries (van den Heuvel 1976). The difference is that one of the two stars, normally the primary, is massive enough to collapse into a BH. When the primary evolves away from the main sequence and expands, it fills its Roche lobe, transfers mass to its companion and eventually its core collapses to form a BH. The system becomes a high-mass X-ray binary (such as Cyg X-1) until the secondary evolves and expands enough to fill its Roche lobe. At this point the mass transfer is almost certainly unstable and the binary goes through a common-envelope phase. The result is a much tighter binary containing the BH and the helium core of the secondary. The last stage involves the supernova explosion and collapse of the helium star into a NS and a BH–NS binary is formed. Variations on this main evolutionary path are possible but detailed calculations show that their relative fraction is negligible (Fryer et al. 1999).

Here we study the formation of BH–NS coalescing binaries, but we consider only their *immediate* progenitors, i.e., systems just before the second core collapse in the binary. There are two reasons for this approach. Modeling the complete evolutionary history of BH–NS binaries is rather uncertain because it involves a long sequence of poorly understood phases, such as non-conservative, stable or unstable mass transfer, wind mass loss from hydrogen- and helium-rich stars, and BH formation with mass loss and possibly kicks. A wide range of assumptions are necessary to describe the evolution and they can affect the results in a complicated way. Instead, we study BH–NS formation for specific pre-SN parameters and we obtain significant constraints on these parameters. This approach frees our calculations from a large set of uncertain assumptions concerning earlier stages. More importantly, it allows us to understand the physical origin of the dependence of our results on the few input parameters, and to examine the robustness of the results.

As described above, we expect that the BH progenitor was the more massive of the two binary members and that the BH formed first in the system. It is in principle possible, through mass transfer episodes, that a mass ratio inversion occurred during the evolutionary history of the system. The result in this case would be that the collapse order was reversed and that the

NS formed before the BH. The immediate BH–NS binary progenitor would then consist of a NS and a non-degenerate star massive enough to collapse into a BH. However, detailed evolutionary calculations covering a wide range of model parameters indicate that the fraction of primordial binaries experiencing such a mass ratio inversion is negligible (Fryer 1999, private communication).

We assume that the orbit before the SN explosion is circular. This is well justified since it is thought that the binary experienced a phase of unstable mass transfer and common-envelope evolution. In principle, one could doubt that this phase occurred, but we will show in § 3.1 that it is actually *necessary* for the formation of *coalescing* BH–NS binaries. In the absence of common-envelope evolution and the resulting orbital contraction, the pre-SN separation would very large ( $\sim 10^3 R_\odot$ ), so that the massive NS progenitor would never fill its Roche lobe. However, we will show that such wide binaries cannot be the progenitors of BH–NS systems tight enough to coalesce within a Hubble time. Given the highly dissipative nature of the common envelope phase, it seems inevitable that the binary orbit will be circularized.

Another inevitable outcome of the mass transfer phases occurring prior to NS formation is the alignment of the spin axes of the BH and NS progenitors with the orbital angular momentum. It is this expectation of alignment that allows us to calculate the spin tilt angle distribution of BH–NS binaries, since we can identify the tilt angle,  $\omega$ , of the post-SN orbital plane relative to the pre-SN plane with the misalignment angle of the BH spin relative to the orbital angular momentum in the BH–NS system (post-SN). We note that it is the BH spin orientation that has been found to be more important in modifying BH–NS inspiral waveforms (Apostolatos et al. 1994).

The results presented in § 3 are obtained under the assumption that kicks imparted to NS are distributed isotropically. In the absence of a clear picture of the physical origin of kicks this assumption seems reasonable. However, for reasons of completeness, we also consider (section 4) the case of non-isotropic kicks that are directed preferentially perpendicular to or in the pre-SN orbital plane.

Finally, in the orbital dynamics analysis presented here we ignore the impact of the supernova shell on the NS companion. This is well justified because the NS companion is a BH with a negligible cross section (even in the case of a non-degenerate  $1 M_\odot$  companion, the impact becomes important *only* if the pre-SN orbital separation  $\lesssim 3 R_\odot$ , see e.g., Romani 1992 and Kalogera 1996).

In our choice of the parameter values for our standard case, a  $10 M_\odot$  BH, a  $4 M_\odot$  NS progenitor, and a  $10 R_\odot$  pre-SN orbital separation, we are motivated by (i) the range of covered by BH mass measurements in soft X-ray transients (Charles 1998), (ii) the general picture of BH–NS formation, according to which their immediate progenitors are the end products of common-envelope evolution, and hence the BH companions have lost their hydrogen-rich envelopes and the orbits are tight ( $\sim 10 R_\odot$ ), and (iii) calculations of the evolution of helium stars with wind mass loss that lead to final masses of  $3 - 4 M_\odot$  (Woosley, Langer, & Weaver 1995) and the results of core-collapse simulations suggesting that helium stars more massive than  $7 - 10 M_\odot$  collapse into black hole instead of a neutron star (Fryer 1999).

## 2.2. Post-Supernova Tilt Angles

We consider a binary consisting of a BH of mass  $M_{\text{BH}}$  and a non-degenerate star (the NS progenitor) of mass  $M_0$  in a circular orbit of separation  $A_0$ . We assume that  $M_0$  explodes instantaneously, i.e., on a timescale shorter than the orbital period, leaving a NS remnant of mass  $M_{\text{NS}}$ , and that a kick of magnitude  $V_k$  is imparted to the remnant. The post-SN characteristics, orbital separation  $A$ , eccentricity,  $e$ , and tilt of the orbital plane  $\omega$ , can be derived based on conservation laws and the geometry of the system (see e.g., Hills 1983; Brandt & Podsiadlowski 1995; Kalogera 1996).

From energy conservation we obtain

$$\alpha \equiv \frac{A}{A_0} = \frac{\beta}{2\beta - u_k^2 \sin^2 \theta - (u_k \cos \theta + 1)^2}, \quad (1)$$

where  $u_k \equiv V_k/V_r$  is the kick magnitude in units of the pre-SN relative orbital velocity  $V_r$

$$V_r = \left( G \frac{M_{\text{BH}} + M_0}{A_0} \right)^{1/2},$$

$\beta$  is the ratio of the total mass after and before the explosion,

$$\beta = \frac{M_{\text{BH}} + M_{\text{NS}}}{M_{\text{BH}} + M_0},$$

and the angles  $\theta$  and  $\phi$  define the direction of the kick:  $\theta$  is the polar angle from the pre-SN orbital velocity vector of the exploding star ( $m$ ) and ranges from  $0 - \pi$  (at  $\theta = 0$ ,  $\vec{V}_k$  and  $\vec{V}_r$  are aligned);  $\phi$  is the azimuthal angle in the plane perpendicular to  $\vec{V}_r$  (i.e.,  $\theta = \pi/2$ ) and ranges from  $0 - 2\pi$  (at  $\theta = \pi/2$  and  $\phi = 0$  or  $\phi = \pi$ , the kick component points along or opposite of the angular momentum axis of the pre-SN orbital plane, respectively; Figure 1).

From orbital angular momentum conservation we obtain for the post-SN eccentricity

$$1 - e^2 = \frac{1}{\beta^2} \left[ u_k^2 \sin^2 \theta \cos^2 \phi + (u_k \cos \theta + 1)^2 \right] \left[ 2\beta - u_k^2 \sin^2 \theta - (u_k \cos \theta + 1)^2 \right]. \quad (2)$$

The tilt angle  $\omega$  between the orbital planes before and after the explosion is equal to the angle between the vector  $\vec{V}_r$  and the projection  $\vec{V}_p$  of  $\vec{V}_r + \vec{V}_k$  onto the plane defined by  $\phi = \pi/2$ , (which contains  $\vec{V}_r$  and is perpendicular to the binary axis). Note that the intersection of the pre- and post-SN planes lies along the binary axis. Evaluating the dot product  $\vec{V}_r \cdot \vec{V}_p$  and using equation (1) we obtain (see also Kalogera 1996)

$$\begin{aligned} \cos \omega &= (u_k \cos \theta + 1) \left[ u_k^2 \sin^2 \theta \cos^2 \phi + (u_k \cos \theta + 1)^2 \right]^{-1/2} \\ &= (u_k \cos \theta + 1) \left( 2\beta - \frac{\beta}{\alpha} - u_k^2 \sin^2 \theta \sin^2 \phi \right)^{-1/2} \end{aligned} \quad (3)$$

For a given set of pre-SN binary parameters (masses and orbital separation) and a fixed kick magnitude, there are only two free parameters in the problem: the kick direction angles  $\theta$  and  $\phi$ . Therefore only two of the post-SN characteristics are truly independent parameters. An assumed distribution  $\mathcal{F}(\theta, \phi)$  for the two kick angles can be transformed into a probability distribution for any two post-SN parameters. Here we are interested in the tilt of the orbital plane so we calculate the Jacobian transformation

$$\mathcal{F}'(\alpha, \omega) = \mathcal{F}(\theta, \phi) \mathcal{J}\left(\frac{\theta, \phi}{\alpha, \omega}\right) = \mathcal{F}(\theta, \phi) \left(\frac{\partial \theta}{\partial \alpha} \frac{\partial \phi}{\partial \omega} - \frac{\partial \theta}{\partial \omega} \frac{\partial \phi}{\partial \alpha}\right), \quad (4)$$

where  $\mathcal{F}'(\alpha, \omega)$  is the probability distribution for  $\alpha$  (eq. [1]) and the tilt angle  $\omega$ .

For an isotropic kick distribution we have

$$\mathcal{F}(\theta, \phi) = \frac{\sin \theta}{2} \frac{1}{2\pi}. \quad (5)$$

Inverting equations (1) and (3) we get

$$\begin{aligned} \cos \theta &= \frac{1}{2u_k} \left( 2\beta - \frac{\beta}{\alpha} - u_k^2 - 1 \right), \\ \sin^2 \phi &= 4 \left[ 4u_k - \left( 2\beta - \beta/\alpha - u_k^2 - 1 \right)^2 \right]^{-1} \left[ 2\beta - \frac{\beta}{\alpha} - \left( \frac{2\beta - \beta/\alpha - u_k^2 + 1}{2 \cos \omega} \right)^2 \right]. \end{aligned} \quad (6)$$

Equations (4) and (5) then give

$$\mathcal{F}'(\alpha, \omega) = \frac{\beta}{2\pi u_k \alpha^2} \left[ \frac{4(2\beta - \beta/\alpha)}{(2\beta - \beta/\alpha - u_k^2 + 1)^2} \cos^2 \omega - 1 \right]^{-1/2} (1 - \cos^2 \omega)^{-1/2} |\cos^{-1} \omega|. \quad (7)$$

Finally, to obtain the probability distribution  $\mathcal{F}_\omega(\omega)$ , we have to integrate  $\mathcal{F}'(\alpha, \omega)$  over  $\alpha$  with appropriate bounds. These bounds are dictated by two requirements: (i) the SN explosion does not disrupt the binary and (ii) the post-SN system is a *coalescing binary*, i.e. it will coalesce within a Hubble time ( $\sim 10^{10}$  yr). Note that the integral of  $\mathcal{F}_\omega(\omega)$  over  $\omega$  is not equal to unity but instead equal to the fraction of BH-NS binaries that satisfy the above two constraints.

### 3. Results

#### 3.1. Limits on the Spin Tilt Angle

Before we go on with the calculation of spin tilt angle distributions, we start by deriving limits on the tilt angle  $\omega$ , given a set of pre-SN parameters ( $M_{\text{BH}}$ ,  $M_0$ , and  $A_0$ ). We derive these limits using equation (7) and imposing the obvious requirements that

$$-1 \leq \cos \theta \leq 1 \quad \sin^2 \phi \leq 1, \quad (8)$$

and that the post-SN system is bound and will coalesce within  $10^{10}$  yr. The latter two constraints translate into limits on the orbital separation  $A$  for a given post-SN eccentricity  $e$  (eq. [2]). Keeping the system bound requires (Flannery & van den Heuvel 1975)

$$\frac{1}{1+e} < \frac{A}{A_0} < \frac{1}{1-e}. \quad (9)$$

The condition that the coalescence time be shorter than  $10^{10}$  yr translates into an upper limit on  $A$  for a given  $e$ . We calculate this limit using expressions derived by Junker & Schaefer (1992) and we plot it in Figure 2, for BH–NS systems and NS–NS systems, for comparison. In this and all subsequent Figures we have adopted  $M_{\text{NS}} = 1.4 M_{\odot}$ , since measured NS masses are all consistent with a narrow range around this value (see Thorsett & Chakrabarty 1998).

The limits on the tilt angle  $\omega$  are shown in Figure 3 as a function of the isotropic kick magnitude,  $V_k$ , and for different values of  $M_{\text{BH}}$ ,  $M_0$ , and  $A_0$ . It is evident that the requirements of equations (8) and (9), and that coalescence occurs within  $10^{10}$  yr, lead to constraints not only on the tilt angle but also on the kick magnitude and the pre-SN separation. The lower limit on kick magnitude arises from the requirement that post-SN systems should coalesce within  $10^{10}$  yr. A minimum kick is necessary to overcome the orbital expansion resulting from the mass loss at NS formation. If there is no kick, or if the kick magnitude is too low, post-SN systems are too wide and have coalescence times longer than  $10^{10}$  yr. The upper limit on kick magnitude arises from both requirements that post-SN systems are bound *and* coalesce within  $10^{10}$  yr. If the kick is too large, then most systems get disrupted, while those that remain bound have wide orbits and long coalescence times. Previous analyses of the effect of kicks on orbital dynamics (e.g., Hills 1983; Kalogera 1996) have shown that formation of post-SN systems that satisfy constraints similar to those considered here require that (i) kick magnitudes be of the order of the pre-SN orbital velocity,  $\sim 500 \text{ km s}^{-1}$  for our standard case, and (ii) kicks be directed close to the orbital plane and opposite to the velocity vector of the exploding star ( $\theta \sim \pi$ ). For a given kick magnitude close to the minimum value required, there is a limit on how large the kick component perpendicular to the pre-SN orbital plane can be. This component is responsible for the tilt of the plane, and hence an upper limit to the plane tilt angle  $\omega$  exists. As the kick magnitude increases and approaches the pre-SN orbital velocity, the range of allowed tilt angles becomes wider. As the kick magnitude increases further and becomes larger than the pre-SN orbital velocity, a lower limit on the tilt angle appears because there is always some excess kick component perpendicular to the pre-SN orbital plane. This qualitative behavior of the allowed tilt angles with an increasing kick magnitude is quite robust and independent of the assumed pre-SN binary parameters. The derived values of the minimum and maximum kick magnitudes depend of course on the values of  $M_{\text{BH}}$ ,  $M_0$ , and  $A_0$  (see Figure 3). For our standard case,  $M_{\text{BH}} = 10 M_{\odot}$ ,  $M_0 = 4 M_{\odot}$ , and  $A_0 = 10 M_{\odot}$ , coalescing BH–NS binaries can be formed only if  $50 \text{ km s}^{-1} < V_k < 1000 \text{ km s}^{-1}$ .

From the discussion above it becomes evident that the range of required kick magnitudes is

determined by

$$V_k \sim V_r = \left( G \frac{M_{\text{BH}} + M_0}{A_0} \right)^{1/2}. \quad (10)$$

Hence the required kick values decrease with increasing  $A_0$ , i.e., for wider and less bound pre-SN binaries. The range of allowed kicks also becomes narrower with increasing  $A_0$  since the pre-SN binary is less bound and is much easier to disrupt once the kick exceeds the orbital velocity. This dependence on  $A_0$  allows us to derive a strong *upper limit* on its value. For the case of  $M_{\text{BH}} = 10 M_{\odot}$ , it must be  $A_0 < 300 R_{\odot}$ . Pre-SN binaries in wider orbits are so loosely bound that the kicks that would allow them to remain bound after the explosion are *too low* to decrease the post-SN orbital separation enough, to make the coalescence time  $< 10^{10}$  yr. Therefore, there is no kick magnitude that allows such wide systems to be both bound and coalescing after the SN.

This upper limit on  $A_0$  is important because it strongly constrains the nature of the NS progenitor. We mentioned above that the NS progenitor is expected on evolutionary grounds to be a helium star, the core of the hydrogen-rich NS progenitor exposed at the end of a common-envelope phase. The derived upper limit on  $A_0$  supports this expectation. Had the NS progenitor just before the SN been a massive, hydrogen-rich star, the orbital separation  $A_0$  would have to be  $\sim 10^3 R_{\odot}$  (e.g., Schaller et al. 1992), to accommodate the radial expansion of the evolved star. For any mass of the NS progenitor appropriate for a hydrogen-rich star ( $10 - 25 M_{\odot}$ , see Fryer & Kalogera 1999), such a configuration can be safely excluded, since the required kick magnitude range vanishes. We conclude, therefore, that immediate BH-NS binary progenitors must contain a BH and a helium-star in orbits with separations  $\lesssim 300 R_{\odot}$ . Such systems can be formed only through a common-envelope phase. Exposure of the helium core through strong mass loss (e.g., Schaller et al. 1992; Wellstein & Langer 1999) can also be excluded for BH-NS progenitors, since the binary orbit expands during such a phase, instead of contracting. Although the upper limit on  $A_0$  is  $\sim 300 R_{\odot}$ , for common-envelope (CE) evolution, the *typical* values of the post-CE orbital separations are much lower,  $\sim 10 R_{\odot}$  (e.g., Kalogera & Webbink 1998).

In agreement with equation (10), an increase in  $M_0$  favors higher kick magnitudes (Figure 3). Here we consider a range of NS progenitor masses appropriate for helium stars. The minimum helium-star mass for NS formation has been estimated to be  $2 - 3 M_{\odot}$  (e.g., Habets 1986) and, based on current core-collapse calculations (Fryer 1999), the upper limit lies probably in the range  $7 - 10 M_{\odot}$ . We plot our results for two values of  $M_0$ ,  $4 M_{\odot}$  and  $10 M_{\odot}$ . It is evident that the dependence of our results on  $M_0$  in such a small range is very weak (Figure 3).

The dependence of the kick and tilt angle limits on the BH mass also follows equation (10), as expected. Here we consider three different values here,  $M_{\text{BH}} = 5, 10$ , and  $20 M_{\odot}$ . We note that, given our present understanding of massive star evolution with mass loss, BH masses in excess of  $\simeq 20 M_{\odot}$  are not favored (Fryer & Kalogera 1999).

In Table 1 we summarize the various sets of pre-SN parameters we consider here, the corresponding pre-SN orbital velocities, and the limits imposed on the isotropic kick magnitude.

### 3.2. Spin Tilt Angle Distributions

#### 3.2.1. Fixed Kick Magnitude

For given values of  $M_{\text{BH}}$ ,  $M_0$ ,  $A_0$ , and  $V_k$ , we calculate the probability distributions of spin tilt angle  $\omega$  for coalescing BH-NS binaries, as described in § 2.2 (integrating Eq. [7] numerically). The results, for our standard case ( $M_{\text{BH}} = 10 M_{\odot}$ ,  $M_0 = 4 M_{\odot}$ , and  $A_0 = 10 R_{\odot}$ ), are shown in Figure 4 (top) for different values of the kick magnitude. Note that in this plot the integral of each distribution is not equal to unity but instead equal to the fraction of post-SN systems that remain bound and will coalesce within  $10^{10}$  yr. We also plot the normalized to unity cumulative angle distributions, i.e., the fraction of systems with tilt angles smaller than a given value  $\omega$ , in Figure 4. The behavior described in § 3.1 is even more clearly seen here. For the case shown in Figure 4, the pre-SN relative orbital velocity is  $V_r \simeq 520 \text{ km s}^{-1}$ . For low kick magnitudes, the tilt angles are restricted to small values. As the kick magnitude increases the allowed range of angles widens and the peak of the angle distribution within this range shifts to its high end. For kicks comparable to or slightly higher than  $V_r$ , tilt angles in the full range from alignment ( $\omega \sim 0^\circ$ ) to anti-alignment ( $\omega \sim 180^\circ$ ) with the orbital angular momentum axis are possible. For even higher kicks the tilts are restricted to only high values ( $> 90^\circ$ , i.e., retrograde post-SN orbits).

#### 3.2.2. Kick Magnitude Distributions

We can take one step further and examine the distribution of BH-NS tilt angles not just for a given kick magnitude but for an assumed distribution of kick magnitudes. The calculation involves the convolution of the previously derived probability distributions of  $\omega$  with a kick magnitude distribution,

$$\mathcal{T}(\omega; M_{\text{BH}}, M_0, A_0) = \int \mathcal{F}_{\omega}(\omega; V_k, M_{\text{BH}}, M_0, A_0) F_K(V_k) dV_k. \quad (11)$$

Since the physical origin of NS kicks is not well understood at present, it is not possible to predict theoretically their magnitude distribution. Instead, there have been several attempts to derive a kick distribution based on observational constraints, primarily from transverse radio pulsar velocity measurements (e.g., Hansen & Phinney 1997; Cordes & Chernoff 1998), but also using other populations (e.g., Fryer, et al. 1998; Kalogera, et al. 1998). A Maxwellian form (Gaussian kick components in all three directions) has often been assumed and the velocity dispersion,  $\sigma$ , can then be fitted to observations. Different  $\sigma$  values have been derived depending on considerations of selection effects and measurement errors for the various NS populations. Overall, a consensus seems to have formed, placing the average kick magnitude in the range  $100 - 500 \text{ km s}^{-1}$ . Here we calculate the final tilt angle distributions for two Maxwellian distributions with  $\sigma = 100, 200$ , and  $400 \text{ km s}^{-1}$ , and for one extreme case of a flat distribution in the range  $0 - 1500 \text{ km s}^{-1}$ . The results are shown in Figure 5 (distribution functions and

normalized cumulative distributions) for our standard case. The dependence of the resulting distribution on the average kick magnitude shows the expected trend, i.e., the higher the average kick, the smaller the fraction of BH–NS binaries with small tilt angles (e.g.,  $\omega < 30^\circ$ ; see Figure 5). The results appear to be remarkably robust in the two cases of a Maxwellian with a relatively high  $\sigma$  and a flat distribution. The origin of this robustness is that the shape of the tilt distribution is not determined by the overall shape of the kick magnitude distribution, but instead by the shape of the distribution (or fraction of kicks) within the range of magnitudes required for BH–NS formation, given the assumed pre-SN parameters.

In Figure 6, we show the dependence of the final tilt distributions for different sets of pre-SN parameters and for a Maxwellian kick distribution ( $\sigma = 200 \text{ km s}^{-1}$ ). It is evident that the fraction of coalescing BH–NS binaries with tilt angles higher than  $30^\circ$  increases as the immediate progenitors becomes more loosely bound.

#### 4. NON-ISOTROPIC KICKS

So far we have assumed that NS kicks are directed isotropically. However, it is possible that certain directions are favored because of the unknown details of the physical mechanism responsible for the kick. In what follows we examine two cases where kicks are preferentially directed either (i) perpendicular to the pre-SN orbital plane along two cones with axes parallel to the pre-SN orbital angular momentum axis and with an assumed opening angle  $\theta_p$  (i.e., *polar* kicks), or (ii) close to the pre-SN orbital plane or else perpendicular to the angular momentum axis in a “fan” shape with an assumed half-opening angle  $\theta_p$  (i.e., *planar* kicks). The angle  $\theta_p$  can vary between  $0^\circ$  and  $90^\circ$ .

These two cases of non-isotropic kicks translate into certain constraints imposed on the two angles  $\theta$  and  $\phi$  that determine the kick direction in the reference frame defined in section §2.1. We derive these constraints using another reference frame, in which the polar angle  $\theta'$  is defined with respect to the pre-SN angular momentum axis (the axis out of the page, towards the reader in Figure 1) instead of  $\vec{V}_r$ . The two frames are connected by the condition

$$\cos \theta' = \sin \theta \cos \phi. \quad (12)$$

For the two cases of anisotropy we consider here, the constraints imposed on  $\theta'$  are

$$\cos \theta_p \leq \cos \theta' \leq 1 \quad \text{and} \quad -1 \leq \cos \theta' \leq -\cos \theta_p, \quad (13)$$

for polar kicks and

$$-\sin \theta_p \leq \cos \theta' \leq \sin \theta_p, \quad (14)$$

for planar kicks. These translate into constraints on  $\theta$  and  $\phi$ :

$$\cos \theta_p \leq |\sin \theta \cos \phi| \leq 1 \quad (15)$$

and

$$0 \leq |\sin \theta \cos \phi| \leq \sin \theta_p, \quad (16)$$

for polar and planar kicks, respectively. The latter two constraints substitute those given in equation (8) for isotropic kicks.

Using equations (15) and (16) we can calculate the limits on the tilt angle  $\omega$  based on the analysis presented in § 2.1. The results are shown in Figure 7 for the case of  $M_{\text{BH}} = 10 M_{\odot}$ ,  $M_0 = 4 M_{\odot}$ ,  $A_0 = 10 R_{\odot}$ , and for angles  $\theta_p$  varying from  $90^\circ$  to  $10^\circ$ . Note that  $\theta_p = 90^\circ$  corresponds to the case of isotropic kicks.

In the case of polar kicks, i.e., kicks constrained in two cones along the orbital angular momentum axis (top panel in Figure 7), the effect of anisotropy is more prominent than in the case of planar kicks, i.e., kicks constrained to be within an angle of the pre-SN orbital plane (bottom panel in Figure 7). This is an indirect demonstration of the fact that, even when all kick directions are allowed, the requirement that post-SN systems are bound in tight orbits acts as a filter and planar kicks are preferred (e.g., Hills 1983; for binary compact objects, see Wex et al. 2000). The top panel of Figure 7 indicates that, as the opening angle of the cones decreases, the range of allowed tilt angles and kick magnitudes shrinks. For the specific choice of masses shown, no coalescing binaries can form if  $\theta_p \leq 30^\circ$ . On the other hand, in the bottom panel, the limits are altered significantly from those in the isotropic case only for  $\theta_p \lesssim 30^\circ$ , when the “fan-shaped” region closes into the pre-SN orbital plane.

The effects of non-isotropic kicks on the range of allowed tilt angles as a function of the kick magnitude (see Figure 7) can be understood based on two considerations: (i) the kick component out of the pre-SN orbital plane is primarily responsible for the tilt, and (ii) bound post-SN systems in tight orbits can be formed only when the pre-SN orbital velocity of the exploding star and the kick component opposite the orbital motion are roughly comparable in magnitude. In the case of polar kicks with low magnitudes, the magnitude of the kick component in the orbital plane becomes restricted. Therefore bound systems are formed with higher and higher tilt angles as the kick anisotropy away from the orbital plane becomes stronger. For moderate magnitudes, very low tilt angles are not allowed for the same reason, but very high tilts are also disfavored because the binaries become either too wide or get disrupted altogether, especially for high total kick magnitudes. As we already mentioned, the effects are less dramatic in the case of planar kicks. Low kick magnitudes tend to favor close binaries with small tilt angles. On the other hand, for large kicks directed within a very small angle from the orbital plane (e.g.,  $10^\circ$ ), the kick component in the plane tends to be too large and systems again become too wide or get disrupted.

In Figure 8 we show the normalized cumulative distributions of tilt angles already convolved with a kick magnitude distribution (Maxwellian with  $\sigma = 200 \text{ km s}^{-1}$ ). As expected based on our understanding, for kicks increasingly restricted in directions away from the pre-SN orbital plane, the fraction of coalescing BH-NS binaries with small tilt angles (for example,  $< 30^\circ$ ) decreases. For kicks increasingly restricted to lie close to the plane, the same fraction increases.

## 5. SUMMARY AND DISCUSSION

We have derived the distribution of tilt angles for coalescing BH–NS binaries using very basic theoretical considerations for BH–NS formation. Our results show that the fraction of systems with tilt angles in excess of  $30^\circ$  ranges from about 30% to 80% with a modest sensitivity to the orbital separation of the BH–NS immediate progenitors and the kick magnitude distribution. Tilt angles in excess of  $50^\circ$ – $100^\circ$  are expected for at most 70% of the coalescing BH–NS. Results obtained by Apostolatos (1995) indicate that aligned templates would be insufficient for more than 50% of all binary orientations if the spin tilt angle exceeds  $30^\circ$ – $40^\circ$  and for *all* binary orientations if the spin tilt angle exceeds  $50^\circ$ – $60^\circ$ . The implication is that the detection rate of BH–NS coalescence events by ground-based laser interferometers (such as LIGO) could be decreased by a factor up to  $\simeq 4$ , if waveform templates for aligned spins are used in the data analysis. It seems reasonable to extend the database to precession-modified templates only for tilt angles in the range  $30^\circ$  to  $50^\circ$ , or at most to  $100^\circ$ . We note that the fraction of coalescing BH–NS with small spin tilt angles increases (decreases) if kicks are preferentially directed perpendicular (close) to the pre-SN orbital plane.

We can also constrain the binary properties of coalescing BH–NS. In particular, we have shown that massive, hydrogen-rich immediate NS progenitors are excluded and that a common-envelope phase is necessary. As a result (i) circular pre-SN orbits and pre-SN spins aligned with the orbital angular momentum axis are expected, and (ii) the pre-SN orbital separations and the NS progenitor masses are restricted to  $A_0 \sim 10 - 100 R_\odot$  and  $M_0 \sim 3 - 10 M_\odot$ . The expectation of pre-SN alignment allows us to identify the tilt of the orbital planes before and after the explosion with the BH spin tilt. The narrow ranges in pre-SN parameters are primarily responsible for the robustness of our results.

Previously, post-SN spin tilt angles have been studied in the context of retrograde orbits in X-ray binaries and their possible connection to long-term periodicities in these systems (Brandt & Podsiadlowski 1995), for BH–NS binaries with a low-mass BH ( $3 M_\odot$ ) and a Roche-lobe filling NS, in the context of precessing jets and their suggested association with gamma-ray bursts (Portegies-Zwart et al. 1999), and for binary BH mergers (Postnov & Prokhorov 1999). Based on the dependence of tilt angles on pre-SN binary parameters and NS kick magnitude our results are in agreement with these studies.

The inspiral waveform of a BH–NS binary is more strongly modified if the spin of the BH (the more massive object in the system) is significantly misaligned with respect to the orbital angular momentum axis. The NS in such systems is not expected to have been recycled in its lifetime (having been formed after the BH). Therefore it would almost certainly be a slow rotator at the time of the inspiral phase and the direction of its spin would have no effect on the waveform. If however, in addition to the BH spin orientation, we were also interested in the spin orientation of the NS, then we would need to make one additional assumption about the physical origin of the NS spin. The generally accepted picture so far has been that the rotation of the NS at birth is determined by the rotation of the collapsing core, and hence the rotation of the NS progenitor.

In this case we would expect the NS spin to be aligned with its progenitor spin, and hence the pre-SN orbital angular momentum axis. The angle  $\omega$  then corresponds to both the BH and the NS spin tilt angle. However, Spruit & Phinney (1998) have argued recently that the origin of the NS spin may be connected to the kick imparted to the NS at birth. Observational and theoretical considerations (Deshpande et al. 2000; Spruit & Phinney 1998; Wex et al. 2000) suggest that the kick timescale must be short enough that the spin axis and kick direction are perpendicular (azimuthal averaging about the spin axis is avoided). Our analysis of the SN orbital dynamics includes the kick direction. Therefore, if the NS spin orientation is of interest, it is possible to use this kick-spin association to calculate the NS spin tilt angle distribution in BH-NS binaries.

Spin-orbit coupling can in principle affect inspiral waveforms of coalescing BH-BH binaries as well. However, as in the case of NS-NS binaries, the effect is expected to be unimportant for equal-mass BH binaries (Apostolatos 1995). It is only when the binary mass ratio is small, as in a typical BH-NS system, that the modification of the waveform can be significant, depending on the tilt angle. In Figure 9, we plot the cumulative spin tilt angle distributions convolved with a kick-magnitude distribution (Maxwellian with  $\sigma = 200 \text{ km s}^{-1}$ ) and assuming isotropic kicks, for two different cases of BH-BH binaries: one containing a  $10 M_\odot$  and a  $5 M_\odot$  BH and another with a  $20 M_\odot$  and a  $10 M_\odot$  BH. Comparison with our results for the standard case (Figs. 5, 6) indicates that BH-BH binaries tend to have small tilt angles. More than  $\sim 90\%$  of the systems have angles smaller than  $30^\circ$ . Therefore, the effects of spin-orbit coupling on BH-BH inspiral waveforms should be rather weak.

We note that in calculating the modifications of the inspiral waveforms in the LIGO frequency band due to the spin-orbit misalignment, knowledge of the spin tilt angles at the time the binary orbit enters the LIGO band is required. The angles we derive in this paper characterize the tilts just after the formation of the coalescing binary. One might worry that gravitational radiation reaction effects could affect the spin orientation as the binary approaches the final inspiral phases. It turns out that, although the spin-orbit coupling is strong enough to modify the waveform within the LIGO band, it is not strong enough to drive tilt angle evolution on a fast timescale. Ryan (1995) showed that the misalignment angles at the time of the formation of the coalescing binary do not change by more than one to a few per cent by the time the system enters the inspiral phases of interest to ground-based laser interferometers.

I am grateful to Bruce Allen and Ben Owen for bringing to my attention the issue of spin orientation and detection of gravitational waves from close BH-NS systems. I would also like to thank H. Apostolatos, S. Hughes, E. Flanagan, and A. Wiseman for discussions on the tilt-angle evolution due to gravitational radiation. I acknowledge full support by the Smithsonian Astrophysical Observatory in the form of a Harvard-Smithsonian Center for Astrophysics Postdoctoral Fellowship.

## REFERENCES

Apostolatos, T.A. 1995, Phys. Rev. D, 52, 605

Apostolatos, T.A., et al. 1994, Phys. Rev. D, 49, 6274

Bethe, H., & Brown, G.E. 1998, ApJ, 506, 780

Brandt, N., & Podsiadlowski, P. 1995, MNRAS, 274, 461

Charles, P.A. 1998, in Theory of Black Hole Accretion Disks, eds. M.A. Abramowicz, G. Bjornsson & J.E. Pringle, (Cambridge: Cambridge University Press), 1

Cordes, J.M., & Chernoff, D.F. 1998, ApJ, 505, 315

Deshpande, A.A., Ramachandran, R., & Radhakrishnan, V. 2000, A&A, in press [astro-ph/9910103]

Flannery, B.P. & van den Heuvel, E.P.J. 1975, A&A, 39, 61

Fryer, C.L. 1999, ApJ, 522, 413

Fryer, C.L., Burrows, A., & Benz, W. 1998, ApJ, 496, 333

Fryer, C.L., & Kalogera, V. 1999, ApJ, submitted

Fryer, C.L., Woosley, S.E., & Hartmann, D.H. 1999, ApJ, in press [astro-ph/9904122]

Habets 1986, Ph.D. Thesis, University of Amsterdam

Hansen, B.M.S., & Phinney, E.S. 1997, MNRAS, 291, 569

Hills, J.G. 1983, ApJ, 267, 322

Hulse, R.A., & Taylor, J.H. 1975, ApJ, 195, L51

Junker, W. & Schaefer, G. 1992, MNRAS, 254, 146

Kalogera, V. 1996, ApJ, 471, 352

Kalogera, V., Kolb, U., & King, A.R. 1998, ApJ, 504, 967

Kalogera, V. & Lorimer, D.R. 2000, ApJ, 530, in press

Kalogera, V., & Webbink, R.F. 1998, ApJ, 493, 351

Lipunov, V.M., et al. 1997, MNRAS, 288, 245

Lyne, A.G., et al. 2000, MNRAS, in press [astro-ph/9911313]

Portegies-Zwart, S.F., Lee, C.-H., & Lee, H.-K. 1999, A&AS, 138, 503

Portegies-Zwart, S., & Yungel'son, L. 1998, A&A, 332, 173

Postnov, K.A., & Prokhorov, M.E. 1999, to appear in the proceedings of *Gravitational Waves and Experimental Gravity*, 1999 Rencontres de Moriond, ed. P. Demarquez, in press [astro-ph/9903193]

Rasio, F.A., & Shapiro, S.L. 1992, ApJ, 401, 226

Romani, R.W. 1992, ApJ, 399, 621

Ruffert, M., et al. 1996, A&A, 311, 532

Ryan, F.D. 1995, PRD, 52, 3159

Schaller, G., et al. 1992, A&AS, 96, 269

Schutz, B.F. 1991, in *the Detection of Gravitational Waves*, ed. D.G. Blair (Cambridge: Cambridge University Press), 406

Spruit, H.C. & Phinney, E.S. 1998, Nature, 393, 139

Taylor, J.H., & Weisberg, J.M. 1982, ApJ, 253, 908

Thorne, K.S. 1996, in *Compact Stars in Binaries* IAU Symp. 165, ed. J. van Paradijs, E.P.J. van den Heuvel & E. Kuulkers (Kluwer Academic Publishers, Dordrecht), 153

Thorsett, S.E. & Chakrabarty, D. 1998, ApJ, 512, 288

van den Heuvel, E.P.J. 1976, in *Structure and Evolution of Close Binary Systems* IAU Symp. 73, ed. P. Eggleton, S. Mitton & J. Whelan (Kluwer Academic Publishers, Dordrecht).

Wellstein, S., & Langer, N. 1999, A&A, 350, 148

Wex, N., Kalogera, V., & Kramer, M. 2000, ApJ, in press [astro-ph/9905331]

Woosley, S.E., Langer, N., & Weaver, T.A. 1995, ApJ, 448, 315

Table 1. Limits on Isotropic Kick Magnitudes

$M_{\text{BH}}$ ( $M_{\odot}$ )	Model Parameters		$V_r$ ( $\text{km s}^{-1}$ )	Minimum Kick ( $\text{km s}^{-1}$ )	Maximum Kick ( $\text{km s}^{-1}$ )
	$M_0$ ( $M_{\odot}$ )	$A_0$ ( $R_{\odot}$ )			
5	4	10	415	120	770
5	10	10	535	240	880
5	4	50	185	135	300
5	10	50	240	190	340
10	4	10	515	50	1035
10	10	10	615	150	1125
10	4	50	230	145	400
10	10	50	275	195	435
20	4	10	675	0	1450
20	10	10	755	0	>1500
20	4	50	300	160	545
20	10	50	340	195	575

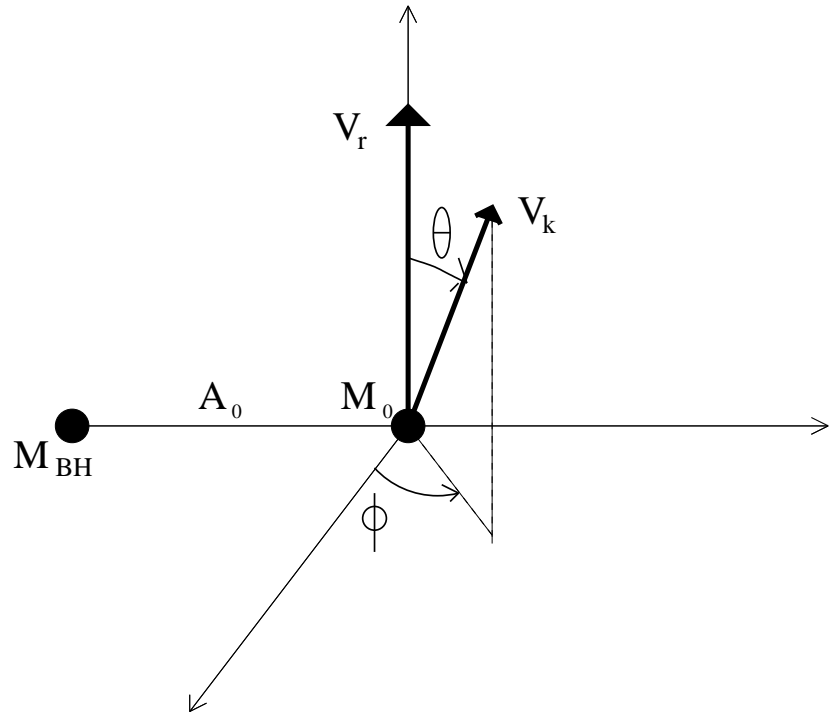


Fig. 1.— Geometry of the binary system consisting of the black hole  $M_{\text{BH}}$  and the NS progenitor  $M_0$  at the time of the supernova explosion. The pre-SN orbital plane coincides with the plane of the page.  $\vec{V}_r$  is the relative orbital velocity in the pre-SN orbit,  $\vec{V}_k$  is the kick imparted to the NS, and the angles  $\theta$  and  $\phi$  define the kick direction.

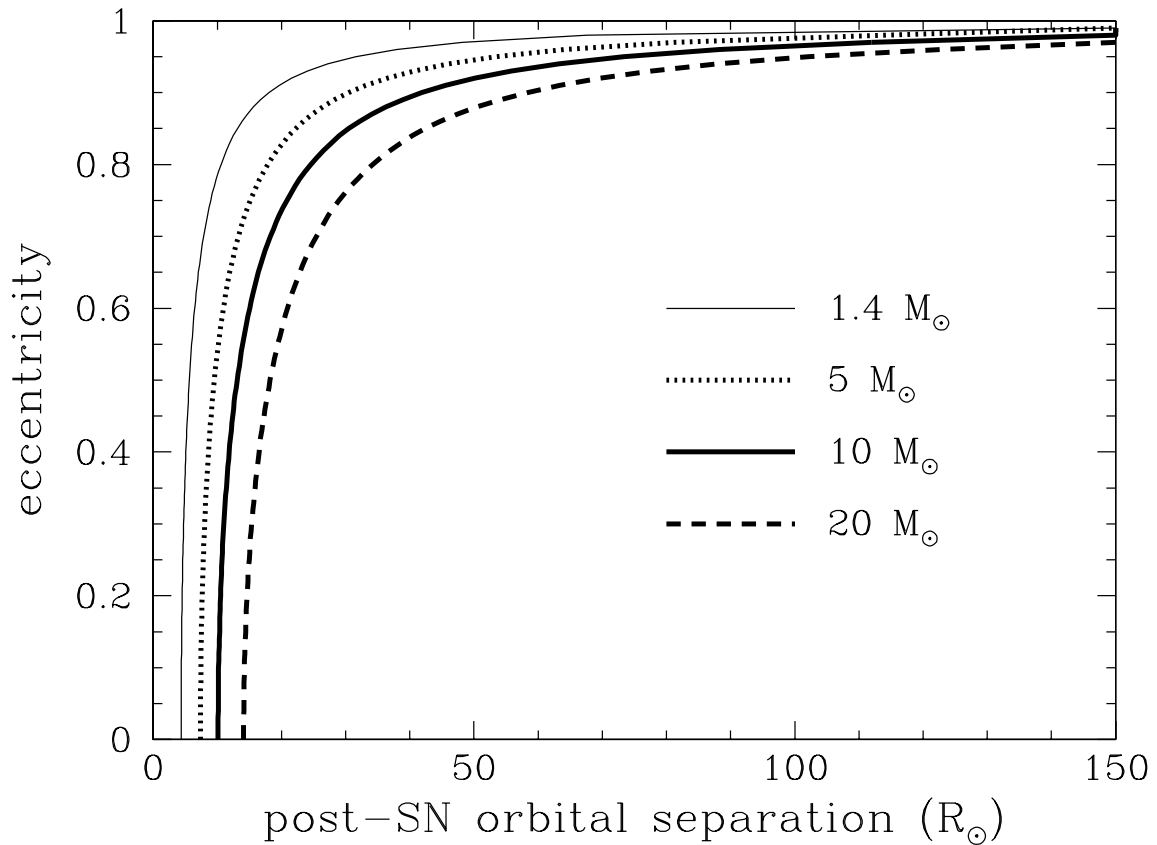


Fig. 2.— Maximum post-SN orbital separation or minimum post-SN eccentricity for coalescence to occur within  $10^{10}$  yr, for NS binaries with NS companions of different masses:  $1.4 M_\odot$  (NS) and  $5, 10, 20 M_\odot$  (BH).

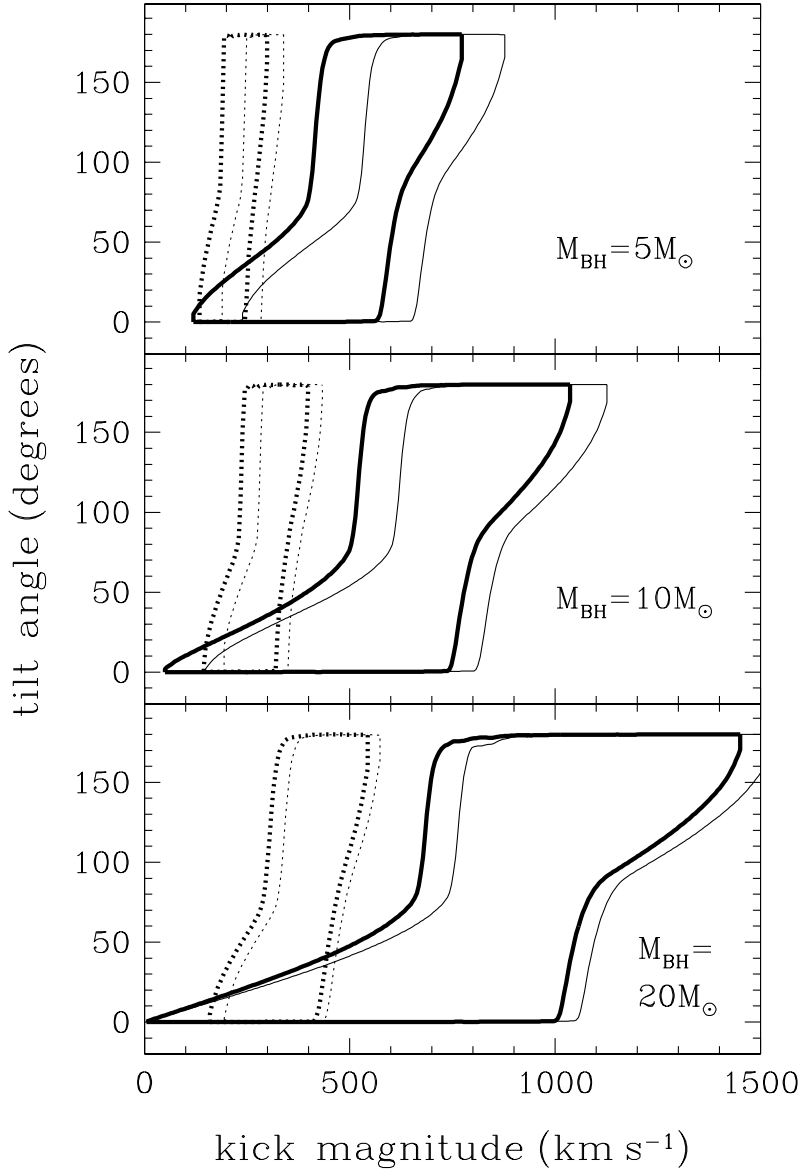


Fig. 3.— Upper and lower limits on the spin tilt angle in coalescing BH-NS binaries as a function of an isotropic kick magnitude, for three different BH masses and for different sets of pre-SN parameters (NS progenitor mass and pre-SN orbital separation):  $4 M_{\odot}$  (thick lines),  $10 M_{\odot}$  (thin lines),  $10 R_{\odot}$  (solid lines), and  $50 R_{\odot}$  (dotted lines).

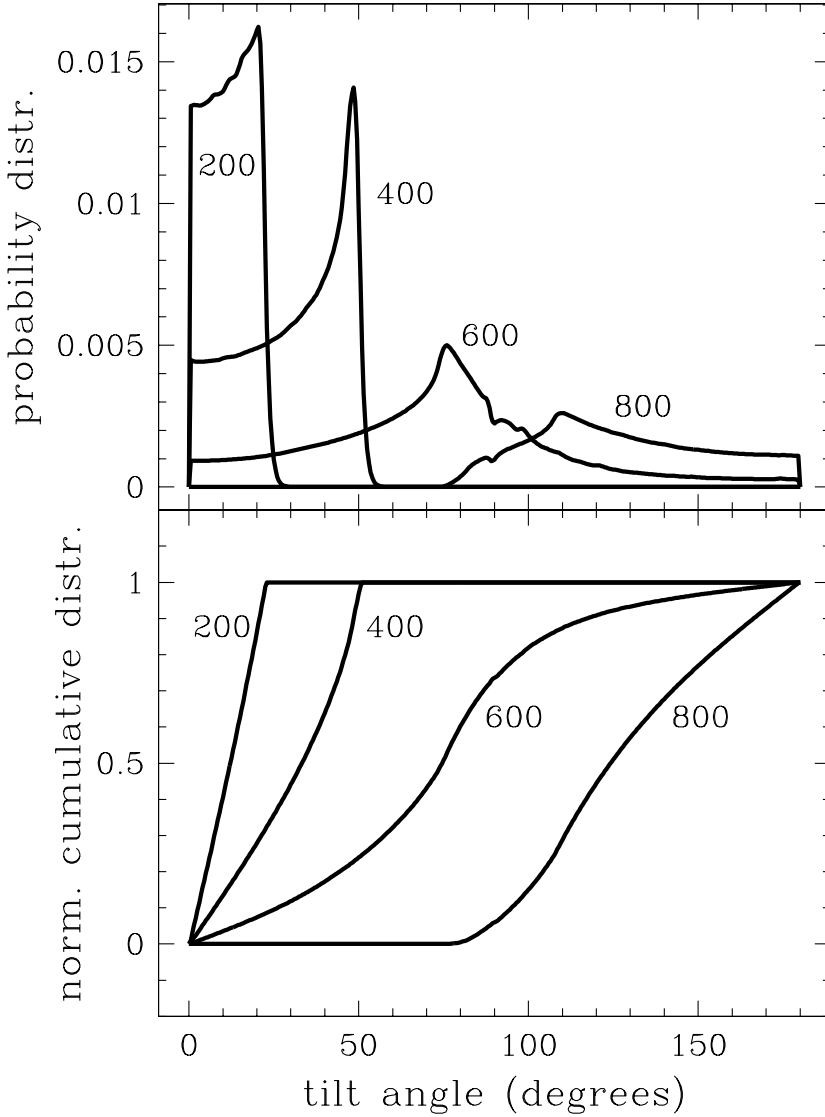


Fig. 4.— Probability distribution (*top*) and normalized (to unity) cumulative distribution (*bottom*) of the spin tilt angle in coalescing BH-NS binaries. Curves are plotted for  $M_{\text{BH}} = 10 M_{\odot}$ ,  $M_0 = 4 M_{\odot}$ ,  $A_0 = 10 R_{\odot}$ , and for four different isotropic kick magnitudes,  $200, 400, 600, 800 \text{ km s}^{-1}$ . Note that the integrals over tilt angle of the distributions in the top panel are equal to the fractions of post-SN systems that remain bound and will coalesce within  $10^{10} \text{ yr}$ .

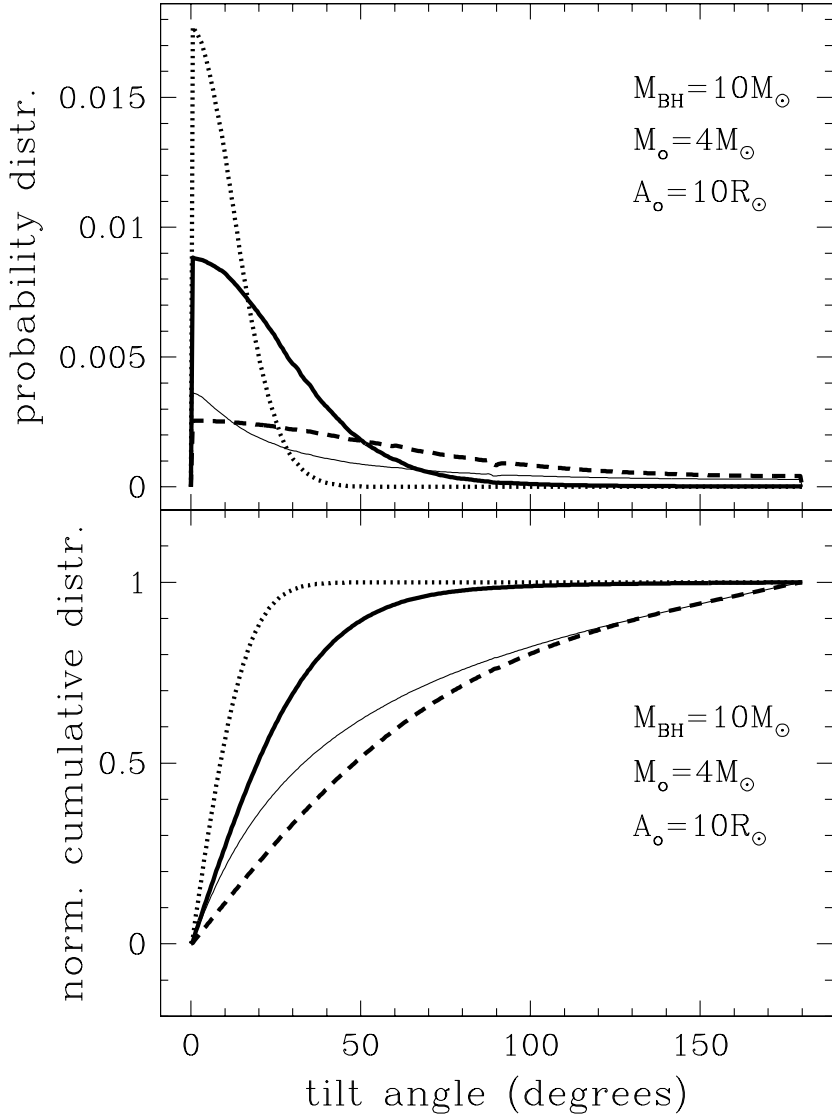


Fig. 5.— Probability distributions (*top*) and normalized cumulative distributions (*bottom*) of the spin tilt angle convolved with four different kick magnitude distributions: Maxwellian with  $\sigma = 100, 200, 400 \text{ km s}^{-1}$  (dotted, solid, dashed lines, respectively) and a flat distribution in the range  $0-1500 \text{ km s}^{-1}$  (thin solid line). Normalization as in Figure 3.

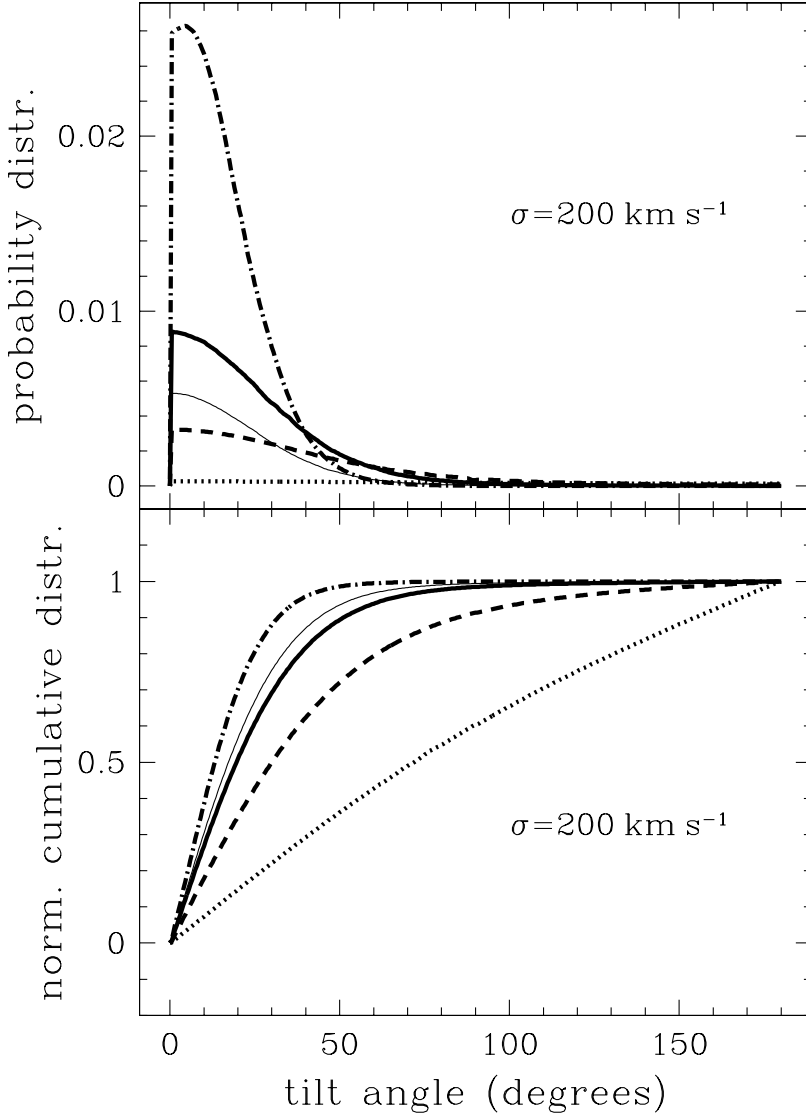


Fig. 6.— Probability distributions (*top*) and normalized cumulative distributions (*bottom*) of the spin tilt angle convolved with a Maxwellian kick magnitude distribution ( $\sigma = 200 \text{ km s}^{-1}$ ), for five different sets of binary parameters:  $M_0 = 4 M_\odot$ ,  $A_0 = 10 R_\odot$ , and  $M_{\text{BH}} = 5, 10, 20 M_\odot$  (dashed, solid, dot-dashed lines, respectively),  $M_{\text{BH}} = 10 M_\odot$ ,  $M_0 = 4 M_\odot$ , and  $A_0 = 50 R_\odot$  (dotted line), and  $M_{\text{BH}} = 10 M_\odot$ ,  $M_0 = 10 M_\odot$ , and  $A_0 = 10 R_\odot$  (thin solid line). Normalization as in Figure 3.

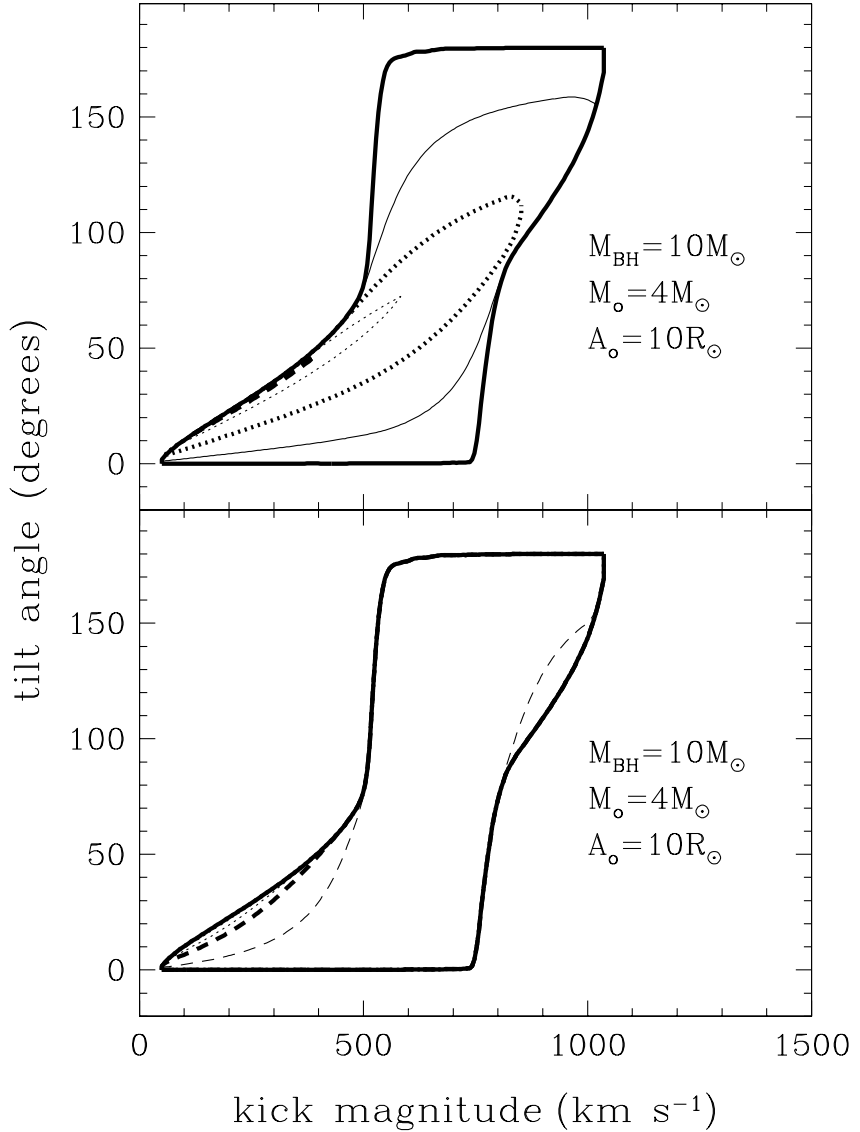


Fig. 7.— Upper and lower limits on the spin tilt angle in coalescing BH-NS binaries as a function of the kick magnitude for  $M_{\text{BH}} = 10 M_{\odot}$ ,  $M_0 = 4 M_{\odot}$ ,  $A_0 = 10 R_{\odot}$ , for polar kicks (*top*) and planar kicks (*bottom*), and for  $\theta_p = 90^\circ, 80^\circ, 60^\circ, 40^\circ, 30^\circ, 10^\circ$  (thick solid, thin solid, thick dotted, thin dotted, thick dashed, and thin dashed lines, respectively).

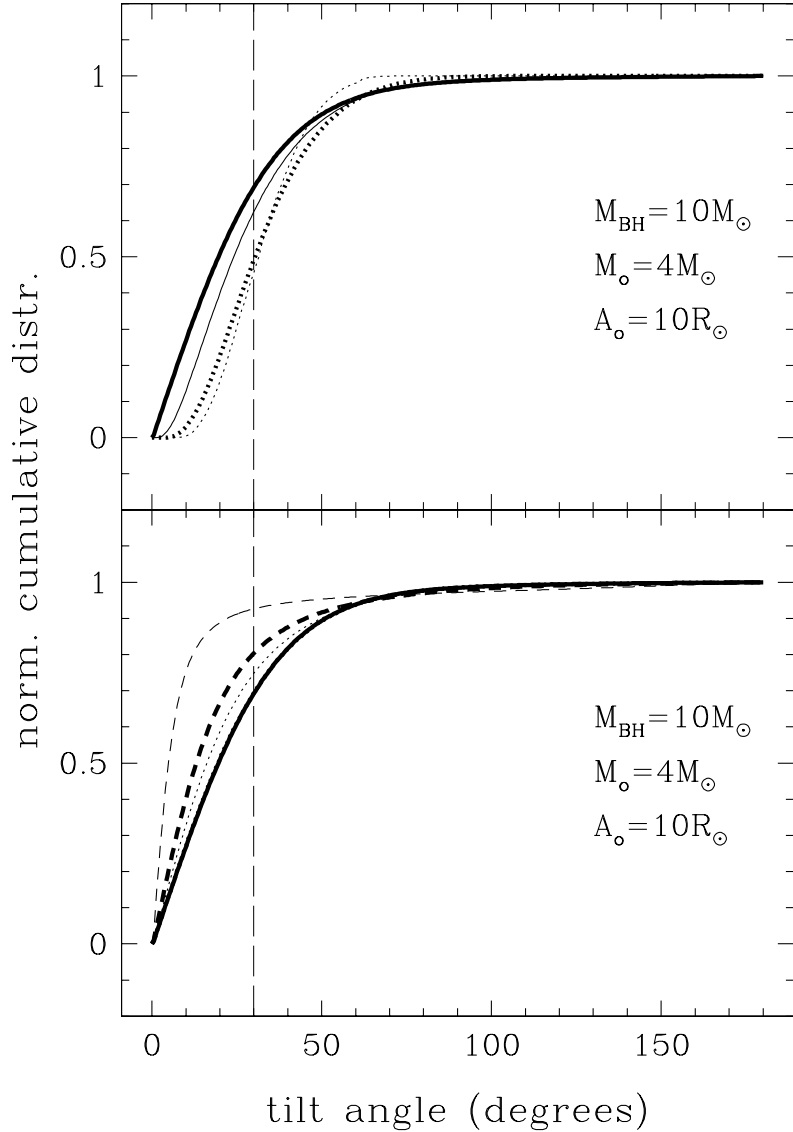


Fig. 8.— Normalized cumulative distributions of the spin tilt angle convolved with a Maxwellian kick magnitude distribution ( $\sigma = 200 \text{ km s}^{-1}$ ), for  $M_{\text{BH}} = 10 M_{\odot}$ ,  $M_{\bullet} = 4 M_{\odot}$ ,  $A_{\bullet} = 10 R_{\odot}$ , for polar kicks (*top*) and planar kicks (*bottom*), and for  $\theta_p = 90^\circ, 80^\circ, 60^\circ, 40^\circ, 30^\circ, 10^\circ$  (line types same as in Figure 7).

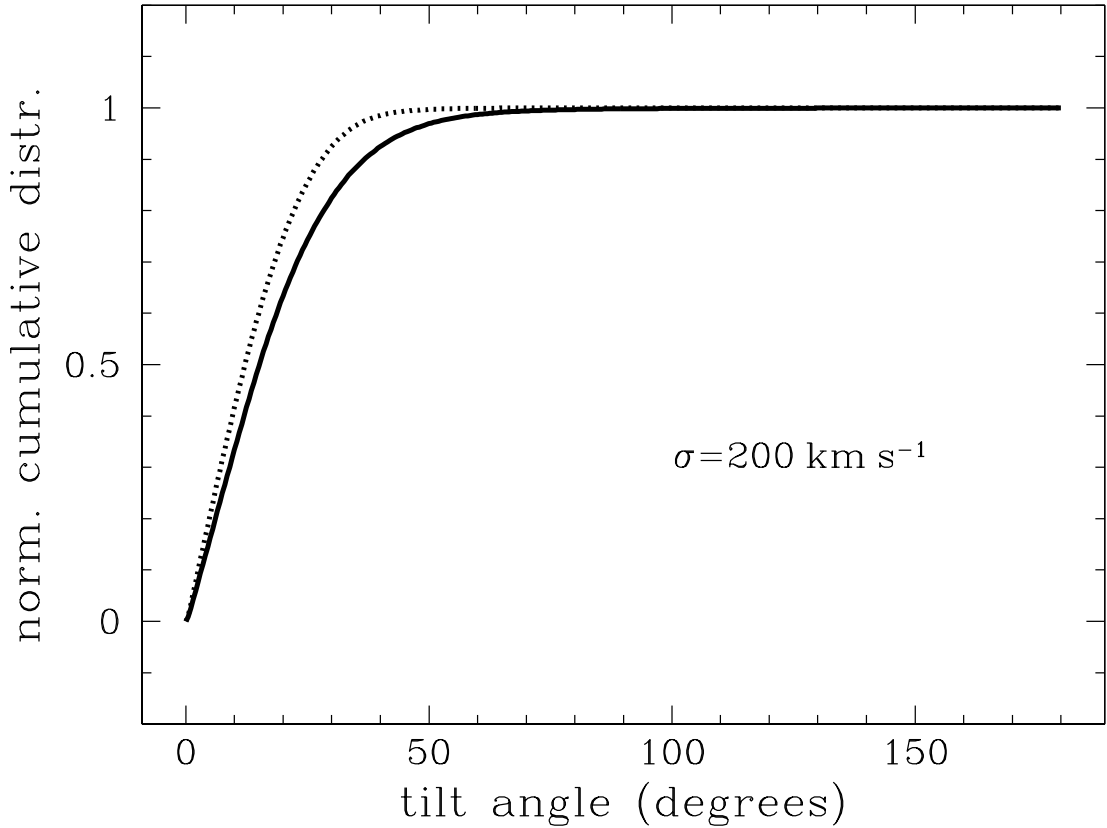


Fig. 9.— Normalized (to unity) cumulative distributions of the spin tilt angle convolved with a Maxwellian kick magnitude distribution ( $\sigma = 200 \text{ km s}^{-1}$ ), for BH–BH binaries:  $M_{\text{BH}}^1 = 10 M_{\odot}$ ,  $M_{\text{BH}}^2 = 5 M_{\odot}$  (solid line),  $M_{\text{BH}}^1 = 20 M_{\odot}$ ,  $M_{\text{BH}}^2 = 10 M_{\odot}$  (dotted line),  $M_0 = 10 M_{\odot}$ , and  $A_0 = 10 R_{\odot}$ . Kicks are assumed to be isotropic.